

¹Jiangsu Key Laboratory for Biodiversity and Biotechnology, College of Life Sciences, Nanjing Normal University; ²School of Biochemical and Environmental Engineering, Nanjing Xiaozhuang University, Nanjing, Jiangsu; ³School of Life Sciences and Food Engineering, Chuzhou University, Chuzhou, Anhui; ⁴School of Ecology, Lishui University, Lishui, Zhejiang, China

Mitochondrial DNA phylogeography reveals a west–east division of the northern grass lizard (*Takydromus septentrionalis*) endemic to China

YAO CAI^{1,2}, JIE YAN¹, XUE-FENG XU³, ZHI-HUA LIN⁴ and XIANG JI¹

Abstract

We sequenced partial mitochondrial DNA from the cytochrome *b* gene (1143 bps) for 385 northern grass lizards (*Takydromus septentrionalis*) from 14 mainland and 14 island populations covering almost the lizard's entire range to examine the influence of geographic barriers (mountain ranges and water bodies) on the diversification of lineages. Phylogenetic analyses revealed a detailed distribution of three evolutionary lineages (W, E and G). Lineage G included individuals exclusively from Guiyang, in the south-western distributional limit. Lineage W included individuals from the central and western parts of the lizard's range on the mainland. Lineage E included individuals from East China, both on the mainland and on islands in the East China Sea. Haplotypes from lineages W and E were co-distributed in Chuzhou and Chibi. The averaged pairwise distance of 6.23% between these lineages indicated a Miocene-Pliocene lineage-split. Lineage E was further subdivided to three sublineages: E1 and E2 comprised of haplotypes from the Zhoushan Islands, and E3 included haplotypes from the eastern mainland, the Zhoushan Islands and two islands south of the Zhoushan Islands. Lineages W and E showed evidence of demographic extensions. The isolation caused by the last transgression (0.01 Ma) has not yet led to a significant genetic differentiation between mainland and island populations in East China. However, divergence among some small islands may be driven by the restriction of migration and genetic drift.

Key words: Lizard – cytochrome *b* – Bayesian analysis – divergence time – genetic drift – Zhoushan Islands – China

Introduction

Our current understanding of the present genetic structure of populations and species is mostly derived from the growing discipline of phylogeography, of which the central goal is to understand how historical biological events have shaped the contemporary distribution and diversity of species (Avice 2000). To infer these events, evolutionary relationships among haplotypes sampled across the geographic distributions of living species are estimated by molecular phylogenetic reconstruction. Mitochondrial DNA studies of widespread species frequently describe levels of intraspecific divergence that correspond to fragmentation/colonization events during Pleistocene or Pliocene (Brown et al. 2002). However, the specific geological and climatic events that have driven phylogeographic patterns within these periods vary depending on the focal region (Liggins et al. 2008). Climatic changes, which were the major environmental changes during Pleistocene glacial–interglacial cycles, have played a key role in shaping genetic diversity of species, and the severe climatic oscillations resulted in great changes in species distributions (Avice 2000; Hewitt 2000, 2004). Southern areas in Europe and North America allowed for the persistence of many species throughout glacial periods, promoting divergence between refugia and the accumulation of genetic diversity within refugium. (Hewitt 2000; Weiss and Ferrand 2007).

In contrast with northern Europe and North America, most of East Asia was never covered by ice sheets and had a relatively mild climate during the Pleistocene (Williams et al. 1998; Ju et al. 2007). Despite these differences, genetic diversity and distribution of species in East Asia have been affected by

environmental changes since the Pleistocene (Lin et al. 2008, 2010; Zhang et al. 2008; Zhao et al. 2011). Moreover, regressions and transgressions of sea level associated with the glacial–interglacial cycle may have influenced the populations and species in coastal areas (Lin et al. 2008; Song et al. 2009; Wei et al. 2010).

The northern grass lizard *Takydromus septentrionalis* is a small oviparous lacertid lizard endemic to China, and has a distributional range covering the central and south-eastern parts of the country (Liu 1999). Within the lizard's range, large mountain ranges and water bodies such as the Luoxiao Mountains, Wuyi Mountains, Qinling Mountains, Yangtze River and Ganjiang River can be found. However, whether these geographic barriers play a role in affecting the diversification of lineages remains unknown. The lizard is locally abundant on the Zhoushan Islands (Ji et al. 1998), which includes some 1300 offshore islands in the East China Sea and can be also found on islands south of the Zhoushan Islands. During the late Pleistocene, the sea level rose and dropped several times in concert with the repeated glacial cycles and, consequently, the Zhoushan Islands had cycles of connection and disconnection with the continent (Wang and Wang 1980). However, whether these processes play a role in influencing lineage sorting of *T. septentrionalis* in its eastern part of distribution remains unknown. In this study, we used the complete mitochondrial cytochrome (*cyt*) *b* gene to investigate the genetic diversity, population structure and evolutionary history of this lizard. Our aims were: (1) to assess the level and partitioning of the genetic variation within *T. septentrionalis*; (2) to compare the phylogeographic pattern of this lizard with that of some other sympatric or co-distributed species such as the Chinese cobra *Naja atra* (Lin et al. 2008) and the five-paced pit-viper *Deinagkistrodon acutus* (Huang et al. 2007) with a 'west–east division' pattern of phylogeography; and (3) to examine the influence of rising-and-dropping cycles of the

Corresponding author: Xiang Ji (xji@mail.hz.zj.cn)

Contributing authors: Yao Cai (flyanter@163.com), Jie Yan (janeiam@163.com), Xue-Feng Xu (xuefxu@chzu.edu.cn), Zhi-Hua Lin (zhlin1015@126.com)

sea level during the late Pleistocene on the current distribution and genetic diversity of the lizard on the Zhoushan Islands.

Materials and Methods

Sampling

We collected 385 individuals from 28 populations covering almost the entire range of *T. septentrionalis*. Fourteen populations were on 14 independent islands in the East China Sea, including two islands (Dongtou and Beiji) south of the Zhoushan Islands. The remaining 14 populations were sampled at different localities on the mainland (Fig. 1). The number of individuals collected from each population and detailed locality information for the populations sampled are given in Table 1.

DNA extraction, amplification and sequencing

Total genomic DNA was extracted from tissue samples that were homogenized in a digestion buffer and proteinase K dissolution. Extractions were performed using standard phenol/chloroform/isoamyl alcohol methods (Sambrook and Russell 2006). The full length of *cyt b* gene was selected for analysis using primers L14910 and H16064 (Busack et al. 2005). The polymerase chain reaction (PCR) was performed as follows in the presence of 3 Mm MgCl₂: 35 cycles of denaturation at 95°C for 30 s, annealing at 54°C for 30 s and extension at 72°C for 50 s. The PCR products were purified and sequenced on an ABI Prism 3700 automated sequencer (Applied Biosystem, Foster City, CA, USA) by Shanghai Sangon Biological Engineering Technology and Service Co. Ltd., with the same primers used for amplification.

Alignment and genetic divergence

The alignment of the concatenated *cyt b* sequences was performed with Clustal_X (Thompson et al. 1997) and corrected by eye. Four lacertid lizards, *Takydromus sexlineatus*, *T. amurensis*, *Eremias brenchleyi* and *Lacerta agilis* (Accession Number GQ142142, GQ142143, EF490071 and GQ142118, respectively), were used as outgroups. The number of haplotypes in each sample site and the values of haplotype diversity and nucleotide diversity were calculated using DnaSP 4.0 (University of Barcelona, Barcelona, Spain; Rozas et al. 2003).

Phylogenetic and phylogeographic analyses

Analyses for phylogenetic inference were conducted using two methods: maximum likelihood (ML) and Bayesian inference (BI). Modeltest

3.7 (Posada and Crandall 1998) and MrModeltest 2.3 (Nylander 2004) were run to determine the appropriate model of molecular evolution based on the Akaike Information Criterion for the ML and BI method, respectively. The BI method was performed with the software MRBAYES (Huelsenbeck and Ronquist 2001) using the GTR + I + G model of substitution. Two independent runs were conducted. Both searches were run with four chains for 10⁷ generations, and the current tree was saved to file every 100 generations. The first 1000 trees sampled were discarded as 'burn-in', as determined by stationarity of lnL assessed using Tracer v. 1.4 (Institute of Evolutionary Biology, University of Edinburgh, Edinburgh, UK; Rambaut and Drummond 2007), and a majority-rule consensus tree generated and posterior probability values calculated from the remaining trees. ML analyses were performed using PHYL 3.0 (Guindon and Gascuel 2003), using a BIONJ tree as starting tree. Branch support was evaluated with non-parametric bootstrap analysis (100 replicates).

Hierarchical analysis of molecular variance (AMOVA) was used to examine the amount of genetic variation partitioned within and among populations using the software ARLEQUIN 3.1 (Zoological Institute, University of Bern, Bern, Switzerland) with significance assessed by 1000 permutations (Excoffier et al. 2005). Various groupings on those populations suggested by the analysis of DNA sequence and geographic distribution were performed. The grouping that reveals maximal value of Φ_{CT} and significantly differs from random organization of similar grouping is assumed to be the most probable geographic subdivisions (Stanley et al. 1996).

To assess the impact of geographic distance on the amount of genetic differentiation between the mainland samples, a Mantel test was carried out using Arlequin 3.1. Genetic distances were based on Slatkin's linearized Φ_{st} values. Geographic distances between populations were calculated based on the latitude and longitude data for each sample site using the Geographic Distance Matrix Generator 1.2.3 (Ersts 2011).

We applied the Bayesian skyline plot (BSP) model by using the software BEAST v1.5.2 (Drummond and Rambaut 2007) to date major demographic changes (such as declines or expansions) and to estimate the magnitude and severity of such events (Heller et al. 2008) in *T. septentrionalis*. As a change-point model, BSP allows us to examine a number of different population sizes through time and use a smoothing procedure to visualize historical population size changes. Using this model, it is possible to plot a population size as far back in time as the most recent common ancestor (MRCA) of a set of sequence samples. The MCMC chain was run with 5×10^7 iterations, and trees were sampled every 1000 iterations. The first 10% of the iterations were discarded as burn-in. Calibration of the molecular clock based on fossils is not possible for *T. septentrionalis* because of the lack of such records. A molecular clock ranging from 0.005 to 0.0125 substitutions per site per million years (corresponding to a

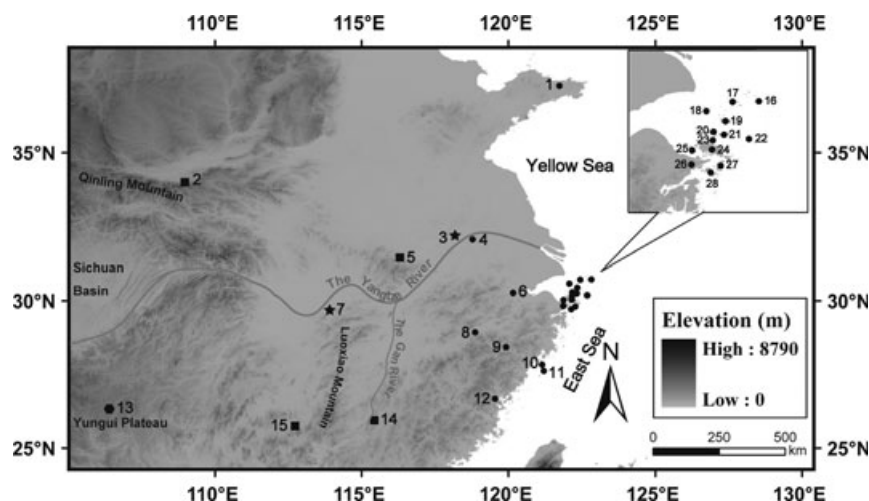


Fig. 1. Sampling sites of *Takydromus septentrionalis* in this study. The numbers in the figure indicate individual populations (see Table 1 for details). The mitochondrial lineages have been labelled by ● for lineage G, ■ for lineage W, and ▲ for lineage E, respectively. Sympatric sites of lineages W and E were labelled by ★

Table 1. Collection data for *Takydromus septentrionalis* specimens used in this study. For each population sampled (alphanumeric locality codes refer to those in Fig. 1), we list collection localities (county, province and exact coordinates), sample sizes subjected to mtDNA examination, the unique mtDNA haplotype numbers and the lineage (W, G, E1, E2 or E3) represented

Code	Locality, Province	<i>n</i>	Lineage	Haplotype no.	Coordinates	<i>h</i>	π [10^2]
1	Yantai, Shandong	14	E3	1–3	37°28'N; 121°74'E	0.385 (0.149)	0.044 (0.019)
2	Chang'an, Shaanxi	14	W1	4–9	34°02'N; 108°97'E	0.791 (0.089)	0.141 (0.028)
3	Chuzhou, Anhui	14	W2, E3	10–14	32°18'N; 118°18'E	0.769 (0.083)	2.567 (0.624)
4	Nanjing, Jiangsu	14	E3	15–19	32°06'N; 118°78'E	0.659 (0.123)	1.000 (0.189)
5	Lu'an, Anhui	14	W1	4, 20–24	31°44'N; 116°28'E	0.681 (0.132)	0.403 (0.078)
6	Hangzhou, Zhejiang	14	E3	25–31	30°27'N; 120°16'E	0.901 (0.046)	0.660 (0.169)
7	Chibi, Hubei	14	W1, W2, E3	32–38	29°69'N; 113°90'E	0.890 (0.050)	3.671 (0.351)
8	Quzhou, Zhejiang	14	E3	31, 39–40	28°93'N; 118°87'E	0.560 (0.125)	0.986 (0.192)
9	Lishui, Zhejiang	14	E3	31, 41–46	28°43'N; 119°92'E	0.813 (0.094)	1.081 (0.206)
10	Dongtou, Zhejiang	14	E3	47–53	27°83'N; 121°15'E	0.758 (0.116)	0.778 (0.216)
11	Beiji, Zhejiang	13	E3	54–55	27°62'N; 121°21'E	0.385 (0.132)	0.673 (0.231)
12	Ningde, Fujian	13	E3	56–59	26.68'N; 119°55'E	0.756 (0.070)	0.087 (0.014)
13	Guiyang, Guizhou	13	G	60–61	26°35'N; 106°42'E	0.385 (0.132)	0.034 (0.012)
14	Yudu, Jiangxi	14	W2	62–63	25°96'N; 115°44'E	0.143 (0.119)	0.187 (0.156)
15	Chenzhou, Hunan	14	W2	64–68	25°74'N; 112°73'E	0.593 (0.144)	0.314 (0.099)
16	Shengshan, Zhejiang	14	E1, E3	69–70	30°72'N; 122°82'E	0.143 (0.119)	1.000 (0.832)
17	Shengsi, Zhejiang	14	E1, E3	51, 71–75	30°71'N; 122°45'E	0.681 (0.132)	1.730 (0.717)
18	Dayangshan, Zhejiang	14	E2, E3	76–81	30°58'N; 122°08'E	0.791 (0.089)	0.419 (0.143)
19	Qushan, Zhejiang	14	E1, E3	82–84	30°44'N; 122°35'E	0.604 (0.076)	1.078 (0.779)
20	Daishan, Zhejiang	14	E3	51, 55, 85–88	30°29'N; 122°18'E	0.681 (0.132)	0.856 (0.208)
21	Dachangtu, Zhejiang	14	E1, E3	55, 84–85, 89–90	30°25'N; 122°33'E	0.802 (0.069)	3.669 (0.433)
22	Miaozihu, Zhejiang	13	E1, E2, E3	50, 89, 91–92	30°19'N; 122°68'E	0.423 (0.164)	2.667 (0.948)
23	Xiushan, Zhejiang	14	E1	93–95	30°17'N; 122°17'E	0.538 (0.115)	0.142 (0.028)
24	Dinghai, Zhejiang	12	E1, E3	96–100	30°04'N; 122°16'E	0.727 (0.113)	1.214 (0.900)
25	Jintang, Zhejiang	14	E2, E3	76, 101,	30°03'N; 121°88'E	0.264 (0.136)	0.392 (0.202)
26	Ningbo, Zhejiang	14	E1, E3	102–103	29°83'N; 121°87'E	0.143 (0.119)	1.012 (0.842)
27	Taohua, Zhejiang	13	E1, E3	90, 104–106,	29°81'N; 122°28'E	0.526 (0.153)	1.947 (0.962)
28	Liuheng, Zhejiang	14	E1, E2	90, 107–110	29°72'N; 122°14'E	0.670 (0.126)	2.200 (0.789)
Outgroup							
	<i>Takydromus sexlineatus</i>	1	GQ142142				
	<i>Takydromus amurensis</i>	1	GQ142143				
	<i>Eremias brenchleyi</i>	1	EF490071				
	<i>Lacerta agilis</i>	1	GQ142118				

pairwise genetic distance of 1.0–2.5% per Myr) was used, based on the evolutionary rates of *cyt b* estimated in several lizards studied (Gubitz et al. 2000; Crochet et al. 2004; Poulakakis et al. 2005; Yan et al. 2010).

Divergence time estimation

To estimate the divergence time between the major lineages (except G, see below for details), we used a Bayesian coalescent approach as implemented in the program BEAST v1.5.2. For these analyses, we used the model of evolution identified by MrModeltest and a constant coalescent model for the prior estimate of population growth. The MCMC chain was run with 10^7 iterations, and trees were sampled every 1000 iterations. The first 10% of the iterations were discarded as burn-in. Under these conditions, the MCMC process performed well, achieving good stationarity and yielding large effective sample size (> 200) for estimates of the MRCA and all other parameters. We used a range of sequence divergence rates (1–2.5% per Myr) and conducted runs to compute the average MRCA and credibility intervals as described in the Peking gecko *Gekko swinhonis* (Yan et al. 2010).

Results

Sequence divergence and phylogenetic and phylogeographic analyses

We obtained the full length of 1143 base pairs (bp) of the mitochondrial *cyt b* gene from all 385 specimens studied. The *cyt b* sequences contained no indels. Of the 225 variable sites

(19.7% of the total nucleotide positions), 164 were parsimony informative. A total of 110 unique haplotypes were identified (GenBank Accession Numbers: JF693494–JF693603) among the ingroup sequences. The number of observed haplotypes within populations ranged from two (six populations) to seven (four populations). Estimates of haplotype (*h*) and nucleotide diversity (π) for each population are given in Table 1. The highest values of haplotype and nucleotide diversity occurred in the Hangzhou and Chibi populations, respectively. Relatively high values of nucleotide diversity also occurred in the Dachangtu, Miaozihu and Chuzhou populations. The Yantai, Yudu and Guiyang populations showed a complete lack of genetic diversity.

The 110 haplotypes were clustered in three major lineages with relatively moderate to high support (Fig. 2), named lineage W (0.92/91 = BI posterior probabilities and ML bootstrap values, respectively), E (0.88/69) and G (0.98/87). Lineage W, consisting of sublineages W1 and W2, included all haplotypes from populations in the central and western parts of the lizard's range on the mainland. Lineage E included haplotypes of eastern mainland and island populations. Haplotypes from both lineages were co-distributed in Chuzhou and Chibi. Lineage E could be broken down into three sublineages: E1 (0.96/89) and E2 (0.79/88) comprising haplotypes all from the Zhoushan Islands, and E3 (0.59/54) including haplotypes from the eastern mainland, the Zhoushan

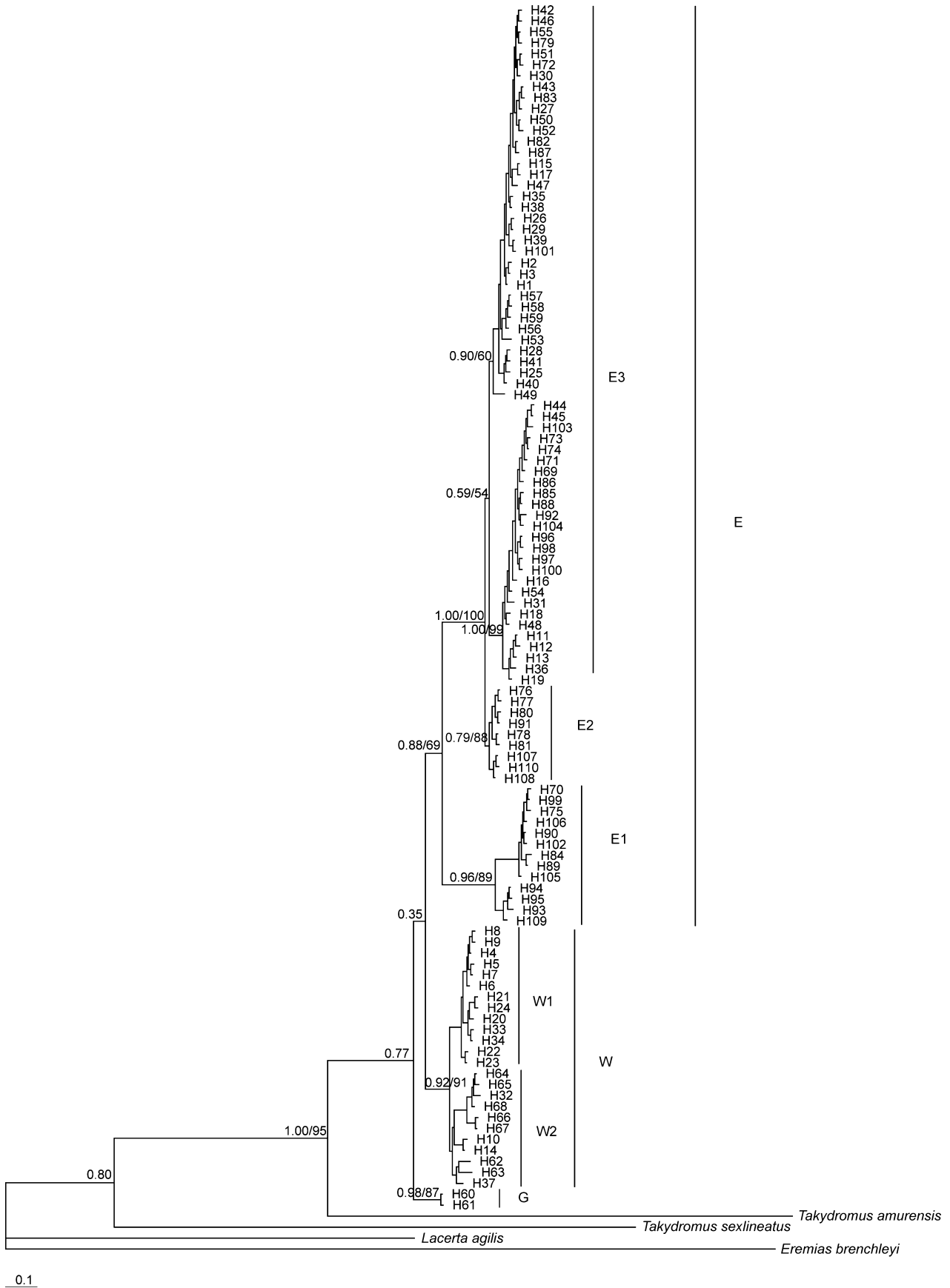


Fig. 2. Genealogical relationships based on cytochrome *b* haplotypes of *Takydromus septentrionalis*. Numbers above the tree branches are the posterior probabilities and bootstrap values for Bayesian inference and maximum likelihood, respectively

Islands and two islands (Dongtou and Beiji) farther south. Sublineages E2 and E3 were clustered as sister groups. Lineage G, composed of the haplotypes from the Guiyang population exclusively, was positioned on the base of the genealogy.

The ML tree was estimated with the best-fit model GTR + G + I (proportion of invariant sites = 0.50; shape parameter $\alpha = 0.9841$; four rate categories). The log-likelihood (-LnL) of the best ML tree obtained was -LnL = 6560.2275. The topologies of the ML and BI trees were similar (dividing into three main clades: W, G and E); therefore, we only present the mean consensus Bayesian tree with posterior probabilities and ML bootstrap values indicating branch support (Fig. 2). The only difference between ML and BI trees was the location of haplotypes from the Guiyang population. In ML tree, Lineage G did not lie at the base of the genealogy and clustered as the sister group to lineage E. Because of the variable positions of lineage G, the BI support for the divergence of lineage W and lineage E was low (Fig. 2).

The sequence divergence (Kimura 2-parameter) among ingroup haplotypes ranged from 0.09 to 8.13%. The mean K2P distance was 6.23% between lineages W and E, 4.24% between lineages W and G, and 5.43% between lineages E and G. The within-group mean K2P distances for lineages W, E and G were 1.43%, 2.75% and 0.09%, respectively.

Table 2 shows results of the AMOVA. The overall differentiation among populations was high and statistically significant ($F_{ST} = 0.72$, $p < 0.0001$). AMOVA revealed that differences among populations accounted for 71.69% of the overall genetic variance observed and that differences within population accounted for 28.31%. The partitions of two groups (lineage G + B versus lineage E) did not get high Φ_{CT} values as expected. When the Chuzhou and Chibi populations were partitioned into the group of lineage E, a slightly higher Φ_{CT} value occurred. The grouping of Chuzhou and Chibi was concordant with the lineage belongings of most of their haplotypes. When populations were clustered into three groups (G, W and E), AMOVA gave a Φ_{CT} value higher than 0.50 ($p < 0.001$); however, this value was still lower. Subdivision of the lineage E made the Φ_{CT} value increase (0.650, $p < 0.001$). This grouping pattern was nearly concordant with the partition of the haplotype lineages (lineage G, W, E2 + E3 and E1) in the mtDNA gene tree. The highest Φ_{CT} value (0.662, $p < 0.001$) emerged when populations were clustered into five groups. In this pattern, populations from the middle

and western mainland were divided into two groups: one for Chang'an and Lu'an, and the other for Chenzhou and Yudu. To test the underlying cause of association between genetic and geographic variation, we performed Mantel tests for the 14 mainland populations, and a significant correlation between mtDNA and geography ($r = 0.528$, $p < 0.01$) was found.

The Bayesian Skyline Plot analysis showed the demographic histories for lineages W and E (Fig. 3). Both lineages had experienced population expansion. For lineage E, a slight decline and a sharp increase occurred at about 0.25 and 0.10 Ma, respectively. For lineage W, the demographic change was relatively stable until an increase occurred at about 0.15 Ma. ESSs were generally high (> 300) for all parameters, indicating stable MCMC inference.

Divergence time

With a mutation rate of 1–2.5% per Myr, the average estimate of the TMRCA was 6.273 Ma (credibility interval between 4.493 and 7.224 Ma), indicating a Miocene-Pliocene split between lineages W and E. The most recent common ancestor (TMRCA) of lineage W was estimated at 1.607 Ma (credibility interval between 1.220 and 1.641 Ma). The average estimate of the TMRCA was 5.847 Ma (credibility interval between 4.165 and 6.689 Ma) between lineages E1 and E2 + E3 and was 1.472 Ma (credibility interval between 1.119 and 1.529 Ma) between lineages E2 and E3. Considering that the position of lineage G in the genealogy was unstable, we did not compute its divergence time.

Discussion

Divergence between major lineages and phylogeographic patterns

The analysis of mtDNA genealogies across the entire range of *T. septentrionalis* revealed a relatively moderate structured pattern of geographic differentiation with the occurrence of three main evolutionary lineages; lineage G restricted to the Guiyang population exclusively, lineage W widespread in the central and western mainland, and lineage E distributed in the eastern mainland and islands in the East China Sea. The average K2P distance between lineage G and W was 4.24%, and 5.43% between lineage G and E. However, lineage G was composed of only two haplotypes detected in 13 individuals

Table 2. Results of analysis of molecular variance for groupings of *Takydromus septentrionalis* estimated using Φ -statistics based on cytochrome *b* sequences

Group compositions [#]	Among groups	Among populations	Within populations	Percentage of variation (%)		
	Φ_{CT}	Φ_{SC}	Φ_{ST}	Among groups	Among populations	Within populations
Two groups (G + W versus E)						
[2, 3, 5, 7, 13–15] [1, 4, 6, 8–12, 16–28]	0.378***	0.650***	0.782***	37.78	40.42	21.80
[2, 5, 7, 13–15] [1, 3–4, 6, 8–12, 16–28]	0.432***	0.641***	0.796***	43.24	36.39	20.37
[2, 5, 13–15] [1, 3–4, 6–12, 16–28]	0.482***	0.636***	0.812***	48.19	32.97	18.83
Three groups (G, W, E)						
[13] [2, 5, 14–15] [1, 3–4, 6–12, 16–28]	0.520***	0.620***	0.818***	52.03	29.74	18.23
Four groups (G, W, E2 + E3, E1)						
[13] [2, 5, 14–15] [1, 3–4, 6–12, 16–20, 24–25, 28][21–23, 26–27]	0.650***	0.427***	0.799***	64.97	14.97	20.06
Five groups (G, W1, W2, E2 + E3, E1)						
[13] [2, 5] [14–15] [1, 3–4, 6–12, 16–20, 24–25, 28][21–23, 26–27]	0.662***	0.406***	0.799***	66.15	13.73	20.12

[#]Locality numbers as in Table 1 are enclosed by square brackets; *** $p < 0.001$. Bold value represents the highest value of Φ_{CT} .

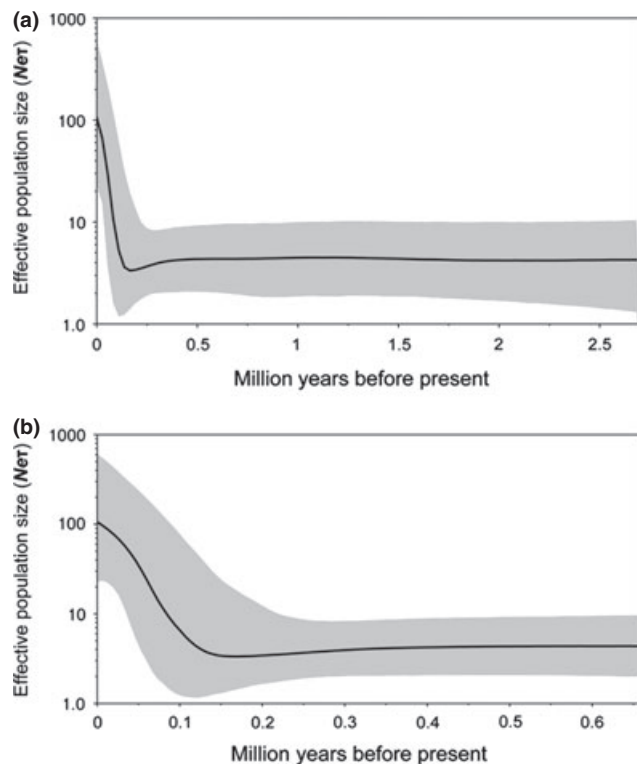


Fig. 3. Bayesian skyline plots. Dark lines represent mean inferred N_e , grey parts mark the 95% highest probability density solid intervals in all panels. (a) For mitochondrial lineage E, and (b) for lineage W

sampled from the Guiyang population, which was too small relative to the haplotypes of lineage E (84) and lineage W (24). This may be responsible for the inconsistent position of lineage G in the BI and ML trees, and more haplotypes of lineage G should improve the phylogenetic resolution. The significant positive correlation between the genetic and geographic distance among mainland populations indicated that isolation by distance was the mainly cause of genetic differentiation in the mainland. For the Guiyang population, the westernmost population, the mountainous area and long distance to other samples can explain the high divergence to both lineage W and lineage E. Lineage W and E were deeply differentiated with a K2P distance of 6.23%, which indicated a Miocene-Pliocene (4.493–7.224 Ma) split between lineages.

The distributions of lineage W and E adjoined in Anhui, Hubei and Jiangxi provinces, in the central-east part of mainland China, indicating a 'west-east division' pattern in this species. Well differentiated evolutionary lineages and similar 'west-east division' have also been reported for *N. atra* (Lin et al. 2008) and *D. acutus* (Huang et al. 2007) based on mtDNA sequence data. However, the presumed physical barriers such as Luoxiao Mts (Lin et al. 2008) and the Ganjiang River (Huang et al. 2007) within the area may not act as barriers to the migration of *T. septentrionalis*. In this study, all the haplotypes from the Yudu population, which is located east to the Luoxiao Mountains and the Ganjiang River, clustered in lineage W.

The mitochondrial DNA data from *G. swinhonis* provided a detailed distribution of two highly divergent evolutionary lineages that coincided with a plate boundary consisting of the Qinling Mountains (Yan et al. 2010). Interestingly, our data showed that the Qinling Mountains may not always act as

barriers to migration. For example, the haplotypes of Chang'an (north of the Qinling Mountains) and Lu'an (south of the Qinling Mountains) were all clustered within lineage W. Furthermore, the two populations shared haplotype 4 (Table 1). The K2P distance and AMOVA results also revealed the same conclusion. It could be possible that the difference in phylogeographic pattern between the two species resulted from their differences in habitat preference and dispersal ability.

Phylogeographic patterns in the Zhoushan Islands

Our phylogenetic results showed that all haplotypes from the Zhoushan area including the Zhoushan Islands and the most adjacent mainland locality, Ningbo, were clustered into three sublineages (E1, E2 and E3). Sublineage E1 included all haplotypes from Xiushan, most haplotypes from Dachangtu, Miaozihu, Ningbo and Taohua, and partial haplotypes from Dinghai and Liuheng. These localities are all situated in the southern part of the Zhoushan Islands. Sublineage E2 consisted of partial haplotypes from Dayangshan, Miaozihu, Jintang and Liuheng, and the remaining haplotypes were intermixed with those from eastern mainland populations in Sublineage E3. The Zhoushan Islands have experienced three transgressions and two regressions since the late Pleistocene, which may have impacted the genetic structure of *T. septentrionalis* distributed in this area. During the second regression, the sea line extended to the edge of the continental shelf, and until 0.02 Ma, the Zhoushan Islands were completely connected with the eastern mainland (Wang and Wang 1980). In the following 5000 years before the third transgression (Wang and Wang 1980), *T. septentrionalis* could easily disperse to any present-day island and gene flow between populations of eastern mainland and present-day islands were allowed. Present-day islands were stabilized approximately 2500 years ago (Wang and Wang 1980), and dispersal barriers (water bodies) between individual islands have formed since that time. The time isolating island and nearby mainland populations is not long for accumulating enough variance to differentiate individual island populations, which is consistent with the topology of Sublineage E3.

Some distinct haplotypes have been detected in the area of the Zhoushan Islands. All these haplotypes were clustered in Sublineage E1 (basal to other eastern haplotypes) and E2 (Fig. 2). Given that most of the islands in Zhoushan are very small and separated from each other, restriction of migration and random genetic drift cannot be precluded as the factors resulting in the differences in haplotype frequency among island populations. The impacts were especially obvious in Xiushan and Daishan. Despite the relatively small geographic distance between Xiushan and Daishan, haplotypes from the two islands were clustered within Sublineages E1 and E3, respectively. It seems likely that, although the disconnection between the Zhoushan Islands and mainland caused by the last transgression (0.01 Ma) has not yet led to significant genetic divergence between mainland and island populations in East China, genetic drift is increasing the divergence among some small island populations.

Acknowledgements

The Provincial Forestry Departments of Anhui, Fujian, Guizhou, Hubei, Hunan, Jiangsu, Jiangxi, Shaanxi, Shandong and Zhejiang provided permits for collecting lizards. This work was supported by

grants from Chinese Ministry of Education (20070319006), Nanjing Normal University Innovative Team Project (#0319PM0902) and Priority Academic Program Development of Jiangsu Higher Education Institutions (CXLX11_0885) to Ji's group. We thank Jian-Fang Gao, Jun Han, Rui-Bin Hu, Hong Li, Long-Hui Lin, Lai-Gao Luo, Yan-Fu Qu, Lin Shu, Xi-Dong Zhang and Qun Zhao for help in animal collection.

Resumen

Fitogeografía en base a ADN mitocondrial revela una división oeste-este de la lagartija de la hierba del norte (Takydromus septentrionalis) endémica de China

En este trabajo se secuenció ADN de una región parcial del gen mitocondrial citocromo *b* (1143 bps) de 385 lagartijas de la hierba del norte (*Takydromus septentrionalis*) provenientes de 14 poblaciones del continente y 14 poblaciones de las islas, cubriendo casi la totalidad de su rango de distribución, a fin de examinar la influencia de las barreras geográficas (distribución de las montañas y cuerpos de agua) en la diversificación de los linajes. Los análisis filogenéticos revelaron una detallada distribución de tres linajes evolutivos (W, E y G). El linaje G incluyó individuos exclusivamente del límite de la distribución sur de Guiyang. El linaje W incluyó individuos del centro y zona oeste de la distribución en el continente. El linaje E incluyó individuos del este de China, tanto del continente como de las islas en el mar Oriental de China. Los haplotipos de los linajes W y E se encontraron codistribuidos en Chuzhou y Chibi. La distancia media entre pares resultó de 6.23% entre los linajes indicando una separación de los mismos ocurrida entre el Mioceno-Plioceno. El linaje E se subdividió posteriormente en tres sub-linajes. E1 y E2 comprendido por haplotipos del este del continente, las islas Zhoushan y dos islas del sur de las islas Zhoushan. Los linajes W y E mostraron evidencias de extensiones demográficas. El aislamiento causado por la última transgresión (0.01 Ma) no muestra aun una diferenciación genética significativa entre las poblaciones del continente y de las islas del Este de China. No obstante, la divergencia entre algunas islas pequeñas podrían deberse a la restricción en la migración y la deriva genética.

References

- Avice JC (2000) *Phylogeography: The History and Formation of Species*. Harvard University Press, Massachusetts.
- Brown R, Suárez N, Pestano J (2002) The Atlas mountains as a biogeographical divide in North-West Africa: evidence from mtDNA evolution in the agamid lizard *Agama impalearis*. *Mol Phylogenet Evol* **24**:324–332.
- Busack SD, Lawson R, Arjo WM (2005) Mitochondrial DNA, allozymes, morphology and historical biogeography in the *Podarcis vaucheri* (Lacertidae) species complex. *Amphibia-Reptilia* **26**:239–256.
- Crochet PA, Chaline O, Surget-Groba Y, Debain C, Cheylan M (2004) Speciation in mountains: phylogeography and phylogeny of the rock lizards genus *Iberolacerta* (Reptilia: Lacertidae). *Mol Phylogenet Evol* **30**:860–866.
- Drummond AJ, Rambaut A (2007) BEAST: Bayesian evolutionary analysis by sampling trees. *BMC Evol Biol* **7**:214.
- Ersts PJ (2011) Geographic Distance Matrix Generator (version 1.2.3). American Museum of Natural History, Center for Biodiversity and Conservation. Available from http://biodiversityinformatics.amnh.org/open_source/gdmg. (Accessed on 17 September 2011).
- Excoffier L, Laval G, Schneider S (2005) Arlequin ver. 3.0: an integrated software package for population genetics data analysis. *Evol Bioinform Online* **1**:47–50.
- Gubitz T, Thorpe RS, Malhotra A (2000) Phylogeography and natural selection in the Tenerife gecko *Tarentola delalandii*: testing historical and adaptive hypotheses. *Mol Ecol* **9**:1213–1221.
- Guindon S, Gascuel OA (2003) Simple, fast, and accurate algorithm to estimate large phylogenies by maximum likelihood. *Syst Biol* **52**:696–704.
- Heller R, Lorenzen ED, Okello JB, Masembe C, Siegmund HR (2008) Mid-Holocene decline in African buffaloes inferred from Bayesian coalescent-based analyses of microsatellites and mitochondrial DNA. *Mol Ecol* **17**:4845–4858.
- Hewitt GM (2000) The genetic legacy of the Quaternary ice ages. *Nature* **405**:907–913.
- Hewitt GM (2004) Genetic consequences of climatic oscillations in the Quaternary. *Philos Trans R Soc B* **359**:183–195.
- Huang S, He SP, Peng Z, Zhao K, Zhao EM (2007) Molecular phylogeography of endangered sharp-snouted pitviper (*Deinagkistrodon acutus*; Reptilia, Viperidae) in mainland China. *Mol Phylogenet Evol* **44**:942–952.
- Huelsenbeck JP, Ronquist F (2001) MRBAYES: bayesian inference of phylogenetic trees. *Bioinformatics* **17**:754–755.
- Ji X, Zhou WH, Zhang XD, Gu HQ (1998) Sexual dimorphism and reproduction in the grass lizard, *Takydromus septentrionalis*. *Russ J Herpetol* **5**:44–48.
- Ju LX, Wang HJ, Jiang DB (2007) Simulation of the Last Glacial Maximum climate over East Asia with a regional climate model nested in a general circulation model. *Paleogeogr Paleoclimatol* **248**:376–390.
- Liggins L, Chapple DG, Daugherty CH, Ritchie PA (2008) A SINE of restricted gene flow across the Alpine Fault: phylogeography of the New Zealand common skink (*Oligosoma nigriplantare polychroma*). *Mol Ecol* **17**:3668–3683.
- Lin LH, Zhao Q, Ji X (2008) Conservation genetics of the Chinese cobra (*Naja atra*) investigated with mitochondrial DNA sequences. *Zool Sci* **25**:888–893.
- Lin LH, Ji X, Diong CH, Du Y, Lin CX (2010) Phylogeography and population structure of the Reeves's butterfly lizard (*Leiolepis reevesii*) inferred from mitochondrial DNA sequences. *Mol Phylogenet Evol* **56**:601–607.
- Liu MY (1999) *Takydromus* Daudin 1802. In: Zhao EM, Zhao KT, Zhou KY (eds), *Fauna Sinica, Reptilia (Squamata, Lacertilia)*, Vol2: Science Press, Beijing, pp 257–269.
- Nylander JAA (2004) MrModeltest v2, Program Distributed by the Author. Uppsala University, Evolutionary Biology Centre.
- Posada D, Crandall KA (1998) Modeltest: testing the model of DNA substitution. *Bioinformatics* **14**:817–818.
- Poulakakis N, Lymberakis P, Valakos E, Pafilis P, Zouros E, Mylonas M (2005) Phylogeography of the Balkan wall lizard (*Podarcis taurica*) and its relatives inferred from mitochondrial DNA sequences. *Mol Ecol* **14**:2433–2443.
- Rambaut A, Drummond AJ (2007) Tracer v1.4, Available from <http://beast.bio.ed.ac.uk/Tracer>.
- Rozas J, Sanchez-DelBarrio JC, Messeguer X, Rozas R (2003) DnaSP, DNA polymorphism analyses by the coalescent and other methods. *Bioinformatics* **19**:2496–2497.
- Sambrook J, Russell DW (2006) *The Condensed Protocols From Molecular Cloning: A Laboratory Manual*. Cold Spring Harbor Laboratory Press, New York.
- Song G, Qu Y, Yin Z, Li S, Liu N, Lei F (2009) Phylogeography of *Alcippe morrisonia* (Aves: Timaliidae): long population history beyond late Pleistocene glaciations. *BMC Evol Biol* **9**:143.
- Stanley HF, Casey S, Carnahan JM, Goodman S, Harwood J, Wayne K (1996) Worldwide patterns of mitochondrial DNA differentiation in the harbor seal (*Phoca vitulina*). *Mol Biol Evol* **13**:368–382.
- Thompson JD, Gibson TJ, Plewniak F, Jeanmougin F, Higgins DG (1997) The CLUSTAL_X windows interface: flexible strategies for multiple sequence alignment aided by quality analysis tools. *Nucleic Acids Res* **25**:4876–4882.
- Wang JT, Wang PS (1980) Relationship between sea-level changes and climatic fluctuations in East China since late Pleistocene. *Acta Geogr Sin* **35**:299–312.
- Wei L, Flanders JR, Rossiter SJ, Miller-Butterworth CM, Zhang LB, Zhang SY (2010) Phylogeography of the Japanese pipistrelle bat, *Pipistrellus abramus*, in China: the impact of ancient and recent events on population genetic structure. *Biol J Linn Soc* **99**:582–594.
- Weiss S, Ferrand N (2007) Phylogeography of Southern European Refugia: Evolutionary Perspectives on the Origins and Conservation of European Biodiversity. Springer, Dordrecht.

- Williams MAJ, Dunkerley DL, de Deckker P, Kershaw AP, Chappel J (1998) Quaternary Environments. Arnold, London.
- Yan J, Wang QX, Chang Q, Ji X, Zhou KY (2010) The divergence of two independent lineages of an endemic Chinese gecko, *Gekko swinhonis*, launched by the Qinling orogenic belt. *Mol Ecol* **19**:2490–2500.
- Zhang H, Yan J, Zhang GQ, Zhou KY (2008) Phylogeography and demographic history of Chinese black-spotted frog populations (*Pelophylax nigromaculata*): evidence for independent refugia expansion and secondary contact. *BMC Evol Biol* **8**:21.
- Zhao Q, Liu HX, Luo LG, Ji X (2011) Comparative population genetics and phylogeography of two lacertid lizards (*Eremias argus* and *E. brenchleyi*) from China. *Mol Phylogenet Evol* **58**:478–491.